

OPTICAL THRU X-RAY SINGLE PHOTON IMAGING SPECTROMETER USING SUPERCONDUCTING TUNNEL JUNCTIONS

D.E. Prober, ^a*

Dept. of Applied Physics, Yale University, New Haven, CT 06520-8284

**in collaboration with C. Wilson, K. Segall, L. Frunzio, L. Li, M. Gaidis (presently JPL), S. Friedrich (presently LLL), Yale; D. Schiminovich, B. Mazin, and C. Martin, Caltech; R. Vasquez, JPL; and A. Szymkowiak and S.H. Moseley, GSFC.*

^a funding by GSFC, NASA, and JPL

We outline the basic concepts of the superconducting tunnel-junction detectors (STJs) and the performance limits. The state of present development is presented, along with projections for future developments. The performance approaches the limit due to intrinsic statistics for backtunneling devices, for photon energies $E \leq 1$ keV. The performance should soon approach those limits for energies above 1 keV now that the interaction of device properties and amplifier noise, most relevant in that higher energy range, has become understood. Present performance provides a spectral resolving power of $E/DE = 25$ for the STJ itself at 5 eV, and $E/DE = 400$ at 6 keV. Count rates $\approx 5,000 \text{ s}^{-1}$ with little degradation of energy resolution have been demonstrated. Further improvement of resolution is expected, with a large numbers of pixels. An STJ camera with 36 pixels has been already demonstrated by ESA researchers on the William Herschel Telescope. Applications are reviewed in a separate presentation by A. Peacock.[1]

1. INTRODUCTION

There is great interest in imaging single photon spectroscopy for future NASA missions. Two developing technologies are [2] the superconducting tunnel junction (STJ) [3,4] and the transition edge sensor (TES) [5]. These detectors can operate efficiently for single photon detection and spectroscopy at energies from the infrared to the x-ray, and can be extended to detect power very sensitively into the sub-millimeter range, and possibly do photon counting there as well. [6] A schematic of the STJ operation is shown in [Fig. 1](#). The absorbed photon breaks Cooper pairs (pair binding energy H meV) of the superconducting ground state, forming single electrons (quasiparticles) which are collected through a tunnel junction. The integrated tunneling current of these single electrons, the charge, is proportional to the photon energy. Variation of the collected charge per photon for an ensemble of monochromatic photons determines the energy resolution of the device. This variation can be caused by intrinsic creation statistics, statistics of the device operation, and by amplifier noise. Analogous noise sources apply for the TES

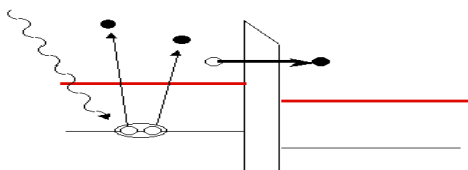
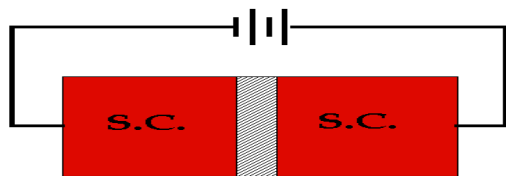


[Fig. 1](#)

In the optical/UV region, attention has focused on imaging single-photon STJ spectrometers. The general approach pursued to date (at ESA) is to use an array of single pixel detectors.[7] STJ detectors with

intrinsic imaging, which use charge-division for imaging, are being developed as well [2,4,7b]. This charge-division imaging is one of the clear advantages of the STJ compared to the TES. There are excellent detailed reviews of the field in the past few years. [2,3] We review here the recent developments and future promise, and provide references to specific papers and reviews. The main research laboratories presently working in this field are at Yale [4], ESA and collaborating groups [3,7,8], Lawrence Livermore Lab (LLL) [9], PSI [10] and Technical Univ. Munich (TUM) [11].

The STJ detector must accomplish at least two functions: absorption of the photon (by a superconducting absorber) and readout of the single-electron excitations (quasiparticles) via a superconducting tunnel junction (STJ). These two functions might be combined into a single absorber-readout film. However, conflicting material requirements and the conflicting requirements of having a large or thick absorber, on the one hand, and fast collection of quasiparticles on the other hand (which requires a small-volume from which to tunnel) lead one to separate the absorbing and tunneling functions. The photon is absorbed, and the quasiparticles are then trapped from the absorber, and then read out. The two main device approaches which result are: 1. a sandwich with the absorber and trap/STJ in a stack (e.g., ESA, LLL), or 2. a lateral separation of the absorber and trap/STJ readout (e.g., Yale). These two approaches are shown in Fig. 1. In Fig. 1 and 2, the leads are not shown.

The sandwich-type devices have been studied extensively at ESA and LLL. Their fabrication borrows the methods of superconducting digital electronics. At Yale we have developed STJ detectors with intrinsic imaging, as seen in Fig. 2, and developed the new microfabrication methods that are required.

Charge-division uses an absorber with lateral trapping and quasiparticle charge division. Such an imaging detector can have many pixels (e50) along the length L of the strip even though a strip uses only two readout STJs. Tests of performance for both types of detectors have been carried out by the respective research groups from H1 to 6,000 eV.

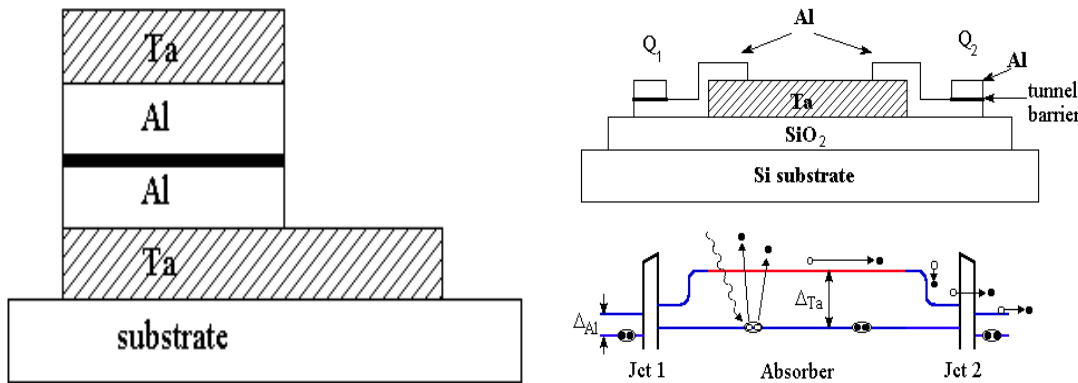


Fig. 2

2. OPERATING PRINCIPLES

A number of physical processes are involved in the operation of the STJ detectors [2,4]. Consider the two-junction device shown in Fig. 2. The incident photon is absorbed in the Ta film, breaking Cooper pairs and creating quasiparticles with charge Q . These quasiparticles rapidly ‘cool’ (in H ns) to the Ta gap energy (0.7 meV), and diffuse at that energy until they reach the Al ‘trap’. In the Al, they can scatter inelastically, losing energy (cooling) until they reach the Al gap (0.18 meV). Once the quasiparticles in the Al trap scatter below the gap of Ta, they are “trapped” in the Al electrode. The quasiparticles then tunnel to the Al ‘counterelectrode’ and this is sensed as an increase in current. This tunneling must occur in a time $d 10^3$ ’s of μ s, as the recombination time to reform pairs (and lose quasiparticles) is Hms. The current pulse is integrated to obtain the charge from each junction, Q_1 and Q_2 :

$$Q = Q_1 + Q_2 \approx 0.6 e (E / \Delta_{Ta}) \quad [1]$$

where E is the photon energy and Δ_{Ta} is the gap energy of Ta. (The energy which does not produce quasiparticles goes into phonons.) The photon energy is deduced from Eq. 1, with the exact proportionality measured in experiment. Variations in Q due to creation statistics set the intrinsic energy width. The energy

width (fwhm) for creation statistics is

$$\Delta E = 2.35 [E e F]^{1/2} \quad \text{creation statistics, with } F = 0.2, \text{ the Fano factor} \quad [2]$$

There is additional statistical broadening due to the trapping process if the charge multiplies upon trapping, and due to backtunneling multiplication (discussed below). Trapping noise can be eliminated with material choice. The backtunneling multiplication for a symmetric structure gives a total energy width

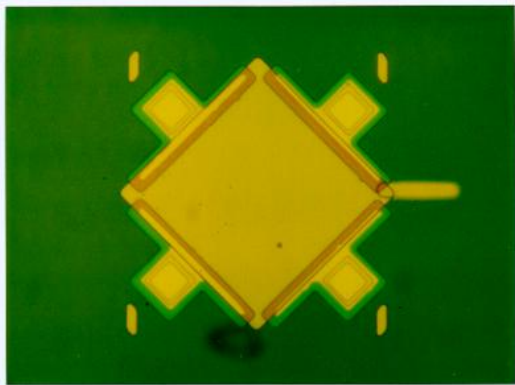
$$\Delta E = 2.35 [E e F_{\text{eff}}]^{1/2} \quad \text{with backtunneling, } F_{\text{eff}} = 1.3 \text{ to } 1.5 \quad [3]$$

Other effects can contribute to the energy broadening. If the charge collection of the tunneling process is incomplete, then there is additional statistical uncertainty – and the effective Fano factor in Eq. 3 is larger.[4] Incomplete cooling of the quasiparticles in the trap, and use of a low bias voltage, give incomplete charge collection.[4a,b]. The amplifier can also contribute current noise, which gives broadening as well. The amplifier noise theory has previously been treated [2] for the case where the amplifier noise simply adds to that of the statistical broadening. This is the correct limit for low photon energy ($E \ll 1$ keV in present devices), but is not a good description at higher photon energies, where the photon-induced tunneling current changes the quiescent I-V curve. For energies above 1 keV, the device interacts with amplifier noise during the current pulse, differently than in the quiescent state. The dynamic resistance during a photon-induced pulse is lower than in the quiescent state, and this leads to an additional broadening due to the interaction of the amplifier voltage noise with the dynamic device characteristics. This case has been studied at Yale by Segall [4] and the new noise mechanisms carefully identified. These new noise mechanisms can be ‘designed out’ of the device by changing to longer tunnel times and biasing the device at a higher voltage. Recent experiments at Yale on x-ray detection at 6 keV show significant improvement in energy resolution when this prescription is followed, as discussed below. With the strip imaging device of [Fig. 2](#), the fraction of charge collected in each junction tells the location of the absorption event. If the photon is absorbed in the center, then the charge divides equally (on average). The formula for the spatial resolution DL along the absorber strip of length L ([Fig. 2](#)) is:

To achieve imaging, one employs either many individual STJs or a strip-imaging device. (A square absorber, with x and y imaging, has also been demonstrated [12] and modeled [13]. Results from Yale fabrication work are shown in [Fig. 3](#).) The charge division statistics should not affect the energy resolution, as all the charge for a strip absorber is collected when Q_1 and Q_2 are summed, in the limit of no absorber loss. We have a spatial resolving power along the

$$\frac{L}{\Delta L} \geq \sqrt{2} \frac{E}{\Delta E}$$

strip given in the formula above for the case where amplifier noise is dominant. When STJ noise is dominant, a similar formula applies.

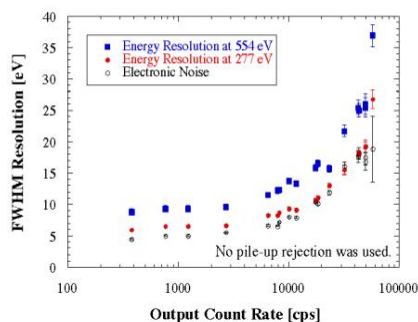


An important process in some STJ designs, and in all sandwich structures, is backtunneling. Consider

[Fig. 3](#)

from the Ta absorber. A quasiparticle can then cycle back and forth across the junction, if there is no path for it to diffuse away after it first tunnels from the trap. This backtunneling process gives a charge which adds to the tunnel current for each traversal of the barrier, due to pair mediation.[2,4] The collected charge is $Q_{\text{backtunneling}} = \langle n \rangle Q$, with Q the created quasiparticle charge, Eq. 1, and $\langle n \rangle$ the number of barrier traversals. $\langle n \rangle$ is typically 3 to 50, and backtunneling thus gives a much larger charge than is created in the absorber. This is advantageous when the charge is small and amplifier noise is relatively large, as for optical photons. However, the statistical noise with backtunneling is a factor of almost 3 larger than without this process; compare Eq. 2 and 3. Also, the length of the pulse is increased, by a factor of 3-50. Backtunneling has been employed in all ESA and LLL experiments due to their stacked STJ geometry. Nevertheless, large count rates with little degradation of energy resolution, e 5,000 c/s, are observed by the LLL group, shown in [Fig. 5](#). This large count rate is observed with backtunneling.

Resolution vs. Count Rate

[Fig. 5](#)

0.1 to 0.2 K, though the ESA group has fielded the S-Cam with a base temperature H 0.3 K, using pumped ^3He . The detectors are sensitive to all photons of frequency above $2D_{\text{Ta}}/h$ H 400 GHz. Thus, photons of energy outside the desired band must be excluded. In optical experiments, excluding IR can be a serious challenge; designs are being developed for such cryogenic IR filters.[14] Use of a cold fiber or imaging fiber bundle to couple in visible photons appears to attenuate fully the IR photons in the optical path, but this is not feasible above H 5 eV. TES devices share this feature of long wavelength sensitivity, and in fact are sensitive to photons of all energies, as there is no energy gap in the TES absorber. Semiconductor x-ray calorimeters also use filters to exclude IR photons.[15]

4. RESULTS – ENERGY RESOLUTION AND CHARGE-DIVISION IMAGING

Two device characteristics are important for low noise. First, the STJ must have low dc current to minimize shot noise, and large differential resistance to minimize the contribution of amplifier voltage noise. Second, the absorber film must have low loss for quasiparticles. Ta films achieve this low loss, but only the LLL group has been successful with Nb films. The loss time of the Yale Ta films is e 0.5 ms, which should allow device lengths e 1 mm. Note that Ta is an excellent absorber from the visible to x-ray range (absorption e60% in the full visible range).[3]

The energy resolution of single-pixel devices has been reported for the range 0.6 – 6 eV at ESA, and between 50-70 and 200-1000 eV at LLL. We present the LLL data in [Fig. 4](#). Both groups find good agreement with Eq. 3, for backtunneling, with devices in the sandwich structure. (The LLL devices use Nb films instead of Ta; for Nb, $D_{\text{Nb}} = 1.5$ meV.) The charge is larger than Eq. 1 by a factor of $\langle n \rangle$ due to backtunneling. The amplifiers used in these experiments were room temperature FETs. The amplifier noise is of order the energy width due to statistics, Eq. 3. This indicates that better amplifiers are desired, especially when one tests devices with the smaller charge, Eq. 1, and the smaller energy width, Eq. 2, expected without backtunneling. A cold JFET should achieve E/DE H 45 at 5 eV without backtunneling, and an RF-SET amplifier [16] may achieve the intrinsic value of E/DE H 65 at 5 eV; this appears to be the ideal readout for the optical STJ. We see in [Fig. 4](#) that the theory for the energy resolution is confirmed, at least for

the sandwich structure in [Fig. 2](#).

Quasiparticles diffuse into the Al trap

from the Ta absorber. A quasiparticle can then cycle back and forth across the junction, if there is no path for it to diffuse away after it first tunnels from the trap. This backtunneling process gives a charge which adds to the tunnel current for each traversal of the barrier, due to pair mediation.[2,4] The collected charge is

$Q_{\text{backtunneling}} = \langle n \rangle Q$, with Q the created quasiparticle charge, Eq. 1, and $\langle n \rangle$ the number of barrier

traversals. $\langle n \rangle$ is typically 3 to 50, and backtunneling thus gives a much larger charge than is created in the absorber. This is advantageous when the charge is small and amplifier noise is relatively large, as for optical photons. However, the statistical noise with backtunneling is a factor of almost 3 larger than without this process; compare Eq. 2 and 3. Also, the length of the pulse is increased, by a factor of 3-50. Backtunneling

has been employed in all ESA and LLL experiments due to their stacked STJ geometry. Nevertheless, large count rates with little degradation of energy resolution, e 5,000 c/s, are observed by the LLL group, shown in

[Fig. 5](#). This large count rate is observed with backtunneling.

3. EXPERIMENTAL CONDITIONS

Device fabrication and measurement methods are given in the references.

Typical experiments are conducted at

backtunneling devices below 1 keV.

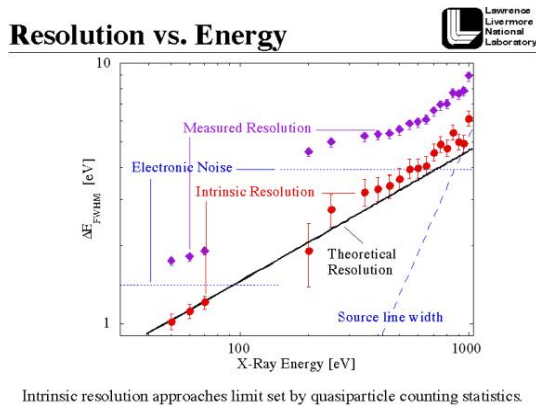


Fig. 4

However, there was a small ‘light leak’ in those experiments, and IR photons, likely from the 77K stage, entered and caused some extra noise. At x-ray energies such light leaks have negligible effect, so we focus on these x-ray experiments in discussing charge division and our energy resolution in imaging detectors.

The x-ray studies at Yale and elsewhere have steadily improved the energy resolution, so that the present ‘record’ is $DE = 12$ to 13 eV fwhm at 5.9 keV, the ^{55}Fe K_{α} line. Recent experiments at Yale [4, Segall, these proceedings] achieved $DE = 13$ eV at $E=6$ keV in June, 2000, as have experiments at TUM with a single Al tunnel junction coupled by phonon transmission to a Pb absorber, which achieves 12 eV.[11] We present the Yale results in Fig. 6, as these also show the charge-division method. The best energy resolution is achieved on a region of the absorber where we can apply the optimal filter; in other regions, the slow diffusion in the Ta absorber smooths the charge pulse. We are working to improve this issue of signal processing. The curvature of the Q_1 vs. Q_2 plot results from the filter used in data processing, not from losses in the Ta strip. Data points at lower energy are due to photon absorptions in the SiO layer which overlies the Ta; this layer was added to protect against oxidation, but is likely needed only over the STJ itself, not over the absorber. Viewed in the histogram of Fig. 6, it is seen that there are few absorption points below the main $K_{\alpha 1}$ - $K_{\alpha 2}$ pair of lines at 5.9 keV. We have measured similar devices (also with SiO protection over the STJ) produced in 1993, over a 6 year period. There is no evidence of aging.

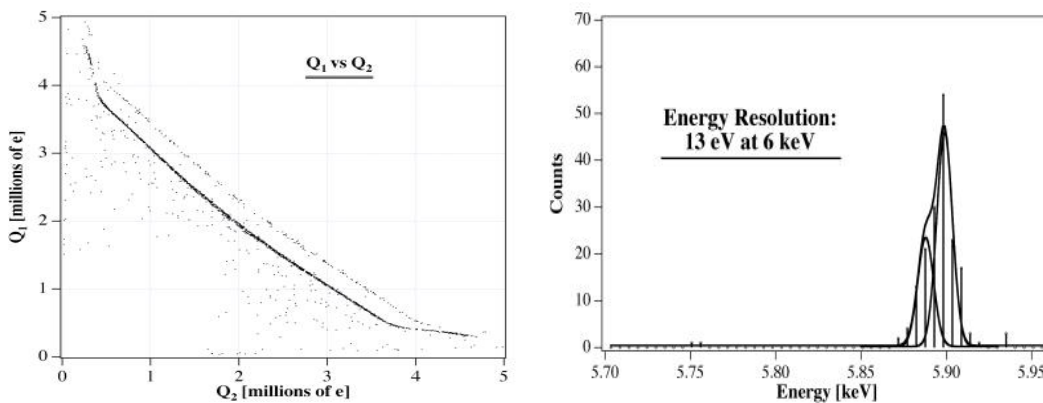


Fig. 6

The x-ray energy resolution is in fact significantly improved over previous Yale devices which achieved $DE = 25$ eV. For those

device designs, Segall accounted carefully for all the noise mechanisms. The newer devices have better energy resolution because the tunnel time is longer than for past devices; also, the geometry was changed to allow biasing at higher voltage. Both these changes ensure that the quasiparticles that enter the trap have longer to cool to get below the energy set by the bias voltage, $(D_{\text{Al}} + eV_{\text{dc}})$. This direction to improve performance was a major conclusion of Segall’s work.[4] The tunnel time of these new devices is about $5 \mu\text{s}$, so that count rates of about 10^4 per sec may be achievable. The previous devices had a tunnel time of order $2 \mu\text{s}$, and were biased at a voltage 40% lower. The improvement of resolution to 13 eV represents a further validation of the modeling done by Segall. Since that modeling provides a prescription for further improvement of performance, we are confident that achieving an energy width of 4 eV is feasible. What will

be required is use of colder temperatures, to reduce the thermal recombination and the shot noise of the dc current, and somewhat slower tunneling. These changes will be introduced in future work.

5. FUTURE DIRECTIONS; COMPARISON TO TES DEVICES

Future goals for STJs are:

1. improved energy resolution of the devices;
2. increased number of pixels beyond the 36 achieved with the S-CAM2, already a significant achievement; and finally
3. cryogenic readout amplifiers, using the RF-SET.

Energy resolution: in the range below 1 keV, STJ single-pixel detectors have achieved the energy width predicted for backtunneling devices, Eq. 3. Further improvement will require the use of devices without backtunneling (and with no other sources of statistical broadening), and such devices –can- be produced with present fabrication methods, using the lateral geometry in [Fig. 2](#). Below 1 keV, one also needs amplifiers with lower noise than present room-temperature JFET amplifiers. Cold FETs will be adequate to achieve device performance where the intrinsic resolution, Eq. 2, is the dominant limit on performance. However, to achieve performance with the fastest count rates and with (potentially) negligible contribution from amplifier noise, the RF-SET transimpedance amplifier [18] will need to be developed. To date, a charge-locked loop RF-SET has been demonstrated,[18] which shows that the periodic characteristics of the device can be used, with feedback, to produce a linear charge amplifier. The STJ requires a current amplifier with low input resistance to collect the full charge and remain biased at the correct dc voltage. This will require development of the transimpedance configuration. This is being pursued by GSFC/Yale.[18]

Improved energy resolution for $E \leq 1$ keV will require a device designed to minimize the noise contributions from the interaction of the amplifier with the STJ in its dynamic state. The work by Segall [4] provides the prescription for this, and is being pursued at Yale. A cold JFET amplifier should be sufficient for these larger photon energies, because of the large charge created. In this energy range, above 1 keV, the absorption coefficient of the strip geometry (with a Ta absorber $H = 1 \mu\text{m}$ thick) is strongly preferred compared to absorption in the stacked-junction geometry, where the absorber is fairly transparent as it is a layer only $H = 0.1 \mu\text{m}$ thick. Moreover, the photons that are not absorbed in the absorber of the strip detector are absorbed in the substrate, and can be easily discriminated by their risetime, and by their charge, which is $1/6$ that of photons absorbed in the absorber. The absorption of the photons which pass thru the absorber in the stacked structure is more complicated. Absorption in the lower Ta film of a stacked junction produces almost the same charge, with the same polarity, as for absorption in the top film. Risetime discrimination is possible for the stacked junction. In the visible range, one may even prefer to couple photons in through the transparent substrate into the bottom film; this approach is followed at ESA, and provides somewhat higher absorption efficiency and some IR attenuation. The resolution is also better, because the bottom film is of higher quality, as it is deposited hot. Coupling in photons through the substrate is not an option for $E \leq 6$ eV.

To achieve a large pixel number (greater than the present 10^2 's of pixels) one can work harder to make more single-pixel (stacked) detectors and room-temperature JFET amplifiers. This approach has been successful for ESA with the 36-pixel S-CAM. While the limits on pixel number in this case are set 'only' by practical considerations, these practical considerations likely limit the number of pixels to of order a few hundred STJs. To achieve more pixels, one needs to employ charge-division (spatial) multiplexing. With charge division, one requires many fewer amplifiers than pixels. The charge division method is now well demonstrated in work at Yale, and recently also at ESA[7] and PSI[10]. There appears to be no penalty for the energy resolution in using charge division. Further work needs to be done to determine quantitatively the loss mechanisms and maximum absorber length set by the absorber losses. With an absorber 1 mm long and 20 microns wide, one can achieve ≈ 50 pixels in the visible range if charge-division statistics are the sole limit on energy resolution. (Creation statistics do not affect the spatial resolution!) We show in [Fig. 7](#) the design of a proposed STJ camera for visible photons, for the Palomar 200 inch telescope. This employs 10 strips, each of which should provide 45 spatial pixels at 5 eV with a cold-FET amplifier for each STJ. This type of camera could probably be extended to have $\approx 10\times$ larger pixel count.

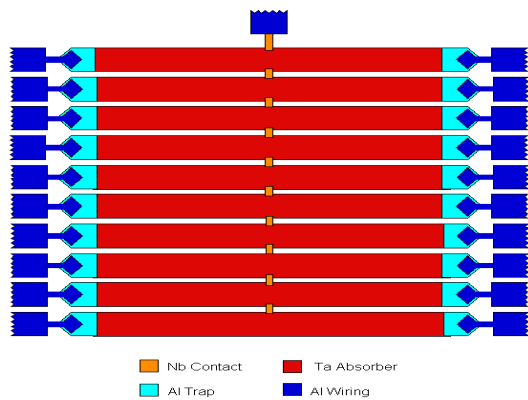


[Fig. 7](#)

Presently, the RF-SET is being developed as a readout amplifier for sub-millimeter direct detectors [6] and as a readout amplifier for STJ single-photon detectors in the visible range [17]. The RF-SET offers better sensitivity for the optical detectors

than cold JFETs (Q is small at low energies), faster response, and the possibility of frequency multiplexing the RF-SET readouts.[18] While it is too early to predict specific performance, we believe that the RF-SET can provide virtually noiseless readout of the STJ, and further can be integrated onto the same chip as the STJ and use much less area than the STJ itself. An attractive feature of the RF-SET amplifier is that it can be frequency multiplexed, so that one rf HEMT amplifier, at 4 K, could process the rf signal from maybe 20 to 50 RF-SETs which are at T_H 0.1 K. This frequency multiplexing has been demonstrated with two frequency channels.[18] While a low frequency feedback line is needed for each RF-SET to read out the STJ, this requirement is not that difficult.. The number of RF-SETs required for a strip-imaging detector is one per STJ. Thus, for the camera shown in [Fig. 7](#), one would require 20 RF-SETs and feedback lines, if one were to use the RF-SET as the STJ readout. It appears that these RF-SETs could all be read out by a single HEMT amplifier, using different drive frequencies (multiplexing) for each RF-SET. This looks tractable.

To conclude, we compare the performance of the STJ and TES: the attractive features of the STJ detector are fast count rate (H 10^4 per sec), energy width ΔE which is reduced (improved) at lower photon energy for a given detector (Eqs. 2 or 3; the TES has a fixed energy resolution for a given device), the capability of spatial charge division, and the future possibility of frequency-multiplexed RF-SET readouts. The STJ is not a thermal device (the TES is), and thus operating the STJ at lower temperatures to improve its resolution does not slow the response. TES detectors, in contrast, tend to be slower, and the very best performance in the x-ray range is achieved with a device with a H ms time constant.[5] TESs to date achieve a resolution comparable to the STJ in the visible range (TESs in the visible are fairly fast [5b]). TESs achieve better resolution (to date) in the x-ray range. STJ energy resolution above 1 keV should improve with our new understanding of the noise mechanisms. For reading out the STJ, the RF-SET is a promising new technology, and is being developed in labs in the US, Europe and Japan. The RF-SET have very broad bandwidth, e 100 MHz. TESs have a mature cryogenic readout technology, the SQUID. The TES can likely use a row-and-column SQUID readout method. This will be first tested with FIR power detectors,[19] where fast response is not as critical as it will be for pulse recording from single photons. It is not certain that this multiplexing method will be fast enough to achieve high readout speeds needed for fast, single photon (i.e., pulse) detection. Clearly, work remains to be done to develop both readout technologies. We conclude that both technologies, the STJ-RF-SET and the TES-SQUID have real promise for single-photon spectroscopic imaging in the range 1 eV to H 10 keV. The recent progress for both technologies is rapid and very encouraging.

REFERENCES

(note – NIMA = Nuclear Instruments and Methods A [444](#) (2000); Proc. of LTD8 Conf.)

1. A. Peacock, these proceedings, and Ref. 3.

2. N.E. Booth and D.J. Goldie, Supercond. Science and Technology **9**, 493 (1996); P. Verhoeve, NIMA [444](#), 435 (2000); radiation hardness of STJ devices is discussed by L. Frunzio et al., Japanese J. Appl. Phys. [37](#), Suppl. 37-2, 40 (1998).

3. N. Rando et al., Proc. SPIE 3435 (1998) and references therein, and Ref. 7a.

4. a. K. Segall et al., Appl. Phys. Lett. 76, 3398 (2000) ; S. Friedrich, Appl. Phys. Lett. 71, 3901 (1977); K. Segall, these proceedings, and K. Segall, Ph.D. Thesis, Yale University, 2000; available from D.Prober; b. Other references, and viewgraphs related to this SADD conference presentation can be found at <http://www.yale.edu/proberlab/> also, C. Wilson, these proceedings.
5. a. K.D. Irwin et al. NIMA 444, 185 (2000) and references therein; the 6 keV response time was 0.7 to 2 ms for the TES; D.A Wollman, et al., NIMA 444, 145 (2000); J. Chervenak et al., Appl. Phys. Lett. 74, 4043 (1999)- SQUID multiplexing.
- 5b. B. Cabrera et al., Applied Physics Letters **73**, 735 (1998); A.J. Miller et al., NIMA 444, 445 (2000), and B. Cabrera, NIMA 444, 304 (2000) and these proceedings.
6. R.J. Schoelkopf et al., IEEE Trans. Applied Supercond. 9, 2935 (1999).
7. a. N. Rando et al., NIMA 444, 441 (2000); P. Verhoeve et al., Appl. Phys. Lett. 72, 3359 (1998); b. charge division is discussed by P. Verhoeve et al., SPIE 4008, (2000); also, R. den Hartog et al., NIMA 444, 278 (2000).
8. C. Nappi et al., Phys. Rev. B58, 11685 (1998) discusses annular junctions.
9. S. Friedrich et al., NIMA 444, 151 (2000) and references therein; J.B LeGrand et al., Appl. Phys. Lett. 73, 1295 (1998); A. Loshaka et al., these proceedings.
10. E.C. Kirk et al, NIMA 444, 201 (2000); Th. Nussbaumer et al., Phys. Rev. B61, 9719 (2000).
11. G. Angloher et al. NIMA 444, 214 (2000), and to be published; H Kraus, et al., Physics Letters B **231**,195 (1989) did early studies of charge division and trapping.
12. R. den Hartog et al., NIMA 444, 278 (2000).
13. L. Li et al, NIMA 444, 228 (2000).
14. N. Rando et al., NIMA 444, 457 (2000), and C. Stahle et al., GSFC, unpublished.
15. F.S. Porter et al., NIMA 444, 220 (2000); M. Galeazzi et al, NIMA 444, 268 (2000), and D. McCammon, these proceedings.
16. R.J. Schoelkopf et al., Science 280, 1238 (1998).
17. D.E. Prober and R.J. Schoelkopf et al, unpublished.
18. T. Stevenson et al., these proceedings and unpublished, and R. Schoelkopf, these proceedings.
19. J. Chervenak, these proceedings.